ERDC/GRL TR-23-1

Geospatial Research Laboratory

US Army Corps
of Engineers®
Engineer Research and
Development Center

ERDC
ENGINEER RESEARCH & DEVELOPMENT CENTER

Army Research, Development, Test and Evaluation

Three-Dimensional Geospatial Product Generation from Tactical Sources, Co-Registration Assessment, and Considerations

Jeffrey G. Ruby, Richard D. Massaro, John E. Anderson, and
Robert L. Fischer

January 2023

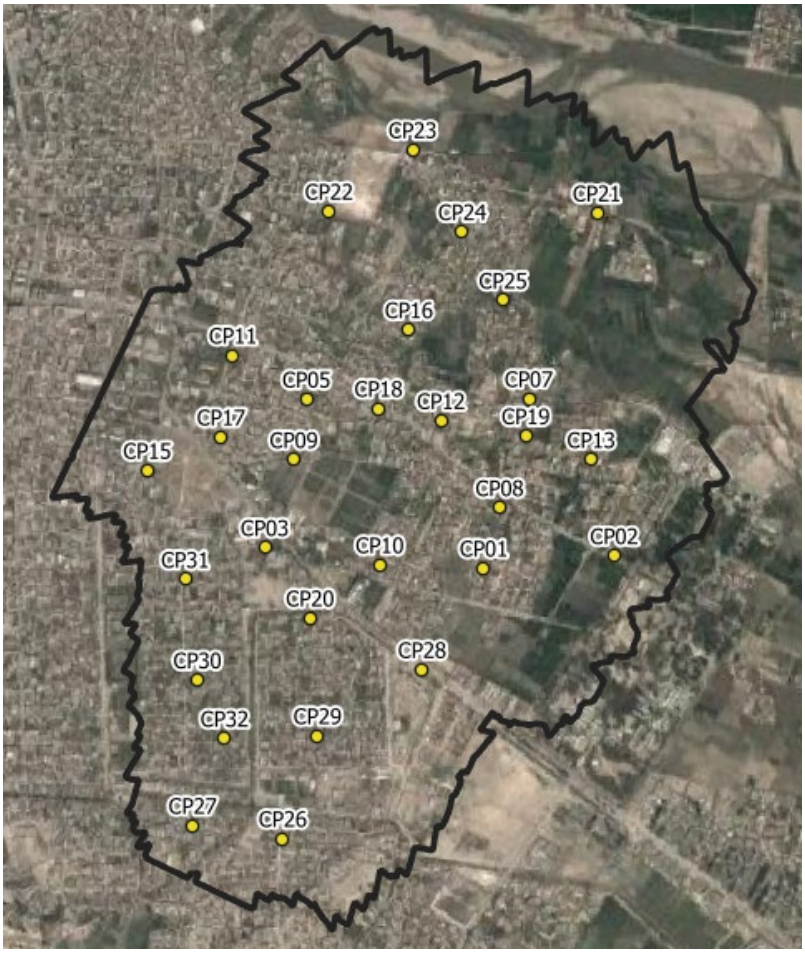

The U.S. Army Engineer Research and Development Center (ERDC) solves the nation's toughest engineering and environmental challenges. ERDC develops innovative solutions in civil and military engineering, geospatial sciences, water resources, and environmental sciences for the Army, the Department of Defense, civilian agencies, and our nation's public good. Find out more at www.erdc.usace.army.mil.

To search for other technical reports published by ERDC, visit the ERDC online library at http://acwc.sdp.sirsi.net/client/default.

Army Research, Development, Test and Evaluation

ERDC/GRL TR-23-1
January 2023

Three-Dimensional Geospatial Product Generation from Tactical Sources, Co-Registration Assessment, and Considerations

Jeffrey G. Ruby, Richard D. Massaro, John E. Anderson

Geospatial Research Laboratory
U.S. Army Engineer Research and Development Center
7701 Telegraph Road
Alexandria, VA 22315

Robert L. Fischer

Strategic Alliance Consulting, Inc.
53A E. Lee Street
Warrenton, VA 20186

Final report

Prepared for U.S. Army Corps of Engineers
Washington, DC 20314-1000

Under PE 0602146A/Project AT7

Abstract

According to Army Multi-Domain Operations (MDO) doctrine, generating timely, accurate, and exploitable geospatial products from tactical platforms is a critical capability to meet threats. The US Army Corps of Engineers, Engineer Research and Development Center, Geospatial Research Laboratory (ERDC-GRL) is carrying out 6.2 research to facilitate the creation of three-dimensional (3D) products from tactical sensors to include full-motion video, framing cameras, and sensors integrated on small Unmanned Aerial Systems (sUAS). This report describes an ERDC-GRL processing pipeline comprising custom code, open-source software, and commercial off-the-shelf (COTS) tools to geospatially rectify tactical imagery to authoritative foundation sources. Four datasets from different sensors and locations were processed against National Geospatial-Intelligence Agency–supplied foundation data. Results showed that the co-registration of tactical drone data to reference foundation varied from 0.34 m to 0.75 m, exceeding the accuracy objective of 1 m described in briefings presented to Army Futures Command (AFC) and the Assistant Security of the Army for Acquisition, Logistics and Technology (ASA(ALT)). A discussion summarizes the results, describes steps to address processing gaps, and considers future efforts to optimize the pipeline for generation of geospatial data for specific end-user devices and tactical applications.

Contents

Figures and Tables

Figures

Tables

Preface

This work was funded under the Army Research, Development, Test and Evaluation (RDT&E) program. The program element number/name is PE 0602146A/Network C3I Technology. The project number/name is AT7/Network Enabled GeoSpatial-GEOINT Services Technology (NEGGS). The report partially satisfies the Knowledge Transition requirement under the NEGGS program as described in the Department of Defense Fiscal Year 2021 Budget Estimates, Army Research, Development, Test and Evaluation—Volume I, Budget Activity 2.

The work was performed by the Information Generation and Management Branch of the Research Division, U.S. Army Engineer Research and Development Center, Geospatial Research Laboratory (ERDC-GRL). At the time of publication of this report, Mr. Michael F. Mailloux was Branch Chief, Mr. Jeffrey B. Murphy was Division Chief, and Mr. Austin Davis was Technical Director. The Deputy Director of ERDC-GRL was Ms. Valerie Carney, and the Director was Mr. David R. Hibner.

COL Christian Patterson was Commander of ERDC, and Dr. David W. Pittman was Director.

This page intentionally left blank.

1 Introduction

1.1 Background

Great power competition presents new challenges to Army and DoD requirements. Future conflicts may involve adversaries with technical capacities that could effectively counter or overmatch existing US and partner capabilities. Army leadership established modernization priorities with associated cross-functional teams in 2017 to meet these challenges (Secretary of the Army 2017; Grinston 2019). Simultaneously, the Army published the Multi-Domain Operations (MDO) Doctrine, which describes how Army Forces will counter and defeat a peer or near-peer adversary in all domains to include air, land, maritime, space, and cyberspace (U.S. Army 2018). An essential component to meet these MDO objectives, and the focus of this work, is the generation and dissemination of timely and accurate geospatial data among all echelons to inform Army commanders and systems.

1.2 Objective

Operations in all domains rely on an accurate common operating picture (COP) derived from maps, imagery, and other two-dimensional (2D) and three-dimensional (3D) spatial data. Commanders require the most accurate and up-to-date geospatial data on which to plan, rehearse, execute, and assess operations. It is challenging to collect, process, exploit, and disseminate these geospatial data within acceptable timelines in an MDO environment, where adversaries may impact our ability to both communicate and maneuver. The problem is further complicated by dynamic battle damage to the terrain itself; infrastructure, transportation, and other critical features may be destroyed, blocked, or otherwise changed in a tactically meaningful way. The ability to rapidly collect, process, and deliver real-time geospatial information as part of the COP is a critical requirement. To meet this need, the Army requires systems and solutions that can deliver geospatial data with the following criteria:

- Quality: Geospatial data and products must be of adequate spatial, radiometric, and temporal resolution to meet the required mission. Applications such as change detection and maneuver will demand multi-date high spatial and radiometric resolution data (pixel

dimension and levels of brightness) so that interpretation tools can provide the required analysis. The ability to define obstacles and identify salient features such as vehicles, doorways, windows, power lines, antennas, alley widths, and wall heights requires specific spatial and radiometric data.

- Speed: Geospatial data products must be produced in tactically meaningful timelines. The traditional approach of processing at Continental United States facilities or centralized tactical operation centers will likely fail in the MDO environment. Raw geospatial data must be processed quickly at local facilities or edge compute devices to ensure immediate exploitation, especially in disconnected, intermittent, and limited (DIL) communication conditions.

- Minimize storage requirements: Imagery, digital surface models (DSMs), and other geospatial products often exist as large data files, especially in native, raw, or preprocessed formats. Methods must be adapted to minimize file sizes without impacting the exploitation potential on the specific end-user applications. All output formats must subscribe to the Standard-Sharable Geospatial Foundation (SSGF) to ensure maximum interoperability across the Army Geospatial Enterprise.

- Accuracy: Potentially the most important attribute with geospatial data, and the primary focus of this work, is the geo-registration accuracy to foundation. Methods that can rapidly and rigorously register tactically collected data across spatial, temporal, and radiometric resolutions are essential. When integrated, these methods allow the fusion of similar and disparate geospatial products to meet mission needs to include targeting, navigation, mobility, and situational awareness.

The collection systems and sensors analyzed in this report represent some of the newest and most flexible platforms capable of delivering geospatial data to US forces. During previous conflicts, space-based or high-altitude sensors operated in partnership with the Intelligence Community provided the majority of the geospatial data; now, an ever-growing fleet of small sensor systems will be employed to build situational awareness in the MDO environment.

1.3 Approach

In this report, multiple fielded sensors from manned and unmanned platforms were studied on their ability to meet spatial accuracy metrics. A specific target objective metric is the capability for recently acquired drone and FMV data products to be co-registered to foundation sources with an accuracy better than 1.0 m in three dimensions (both horizontal and vertical). An important point is that this 1.0 m metric doesn't necessarily mean "absolute" registration to true geodetic coordinates, for instance, as measured from independent GPS-survey points. Rather, this approach is meant to show that the GOTS tools developed by this effort can automatically co-register coarsely controlled, new data to pre-existing foundation products at that 1.0 m level.

1.4 Scope

For this work, COTS drone platforms that use relatively simple, small-format cameras flying on hand-launched, unmanned aircraft were selected for analysis. Drone systems are currently used for both tactical and support missions overseas for multiple programs. Full-motion video (FMV) feeds were also analyzed. FMV sensors are hosted on thousands of fielded tactical and commercial aircraft and represent an underutilized source of raw data for 2D and 3D mapping products.

In addition to analyzing several sensor modalities, multiple geographic sites were selected to help understand the capabilities of these co-registration techniques. Sites selected included a forested piedmont environment, a dense Middle Eastern urban area, an arid US Army training site, and a coastal/littoral region.

2 Photogrammetric Processing Approach

2.1 Structure from motion approach

Structure from motion (SfM) is a new approach to generating 2D and 3D geospatial products from a series of overlapping images. While the mathematical techniques are in principle the same as traditional photogrammetry, the SfM approach solves the camera pose and ground geometry simultaneously using a highly redundant bundle adjustment seeded from matching features in multiple overlapping images (Westoby 2012). The SfM technique has become commonplace with improved access to low-cost drones to generate the data, as well as increases in computer processing power, particularly graphical processing units (GPUs), which perform the mathematics, and open source or low-cost COTS software to process the data.

The SfM software used for this effort was Agisoft Metashape. Metashape is a popular, commercial, small-UAS mapping processing software package. Metashape is well suited for creation of terrain surfaces, orthometric mosaics, as well as three-dimensional (3D) models. Metashape is available as a standalone product but can also be bundled with hardware during the acquisition of the aircraft. Other positive points include the ability to script using Python and execute via a command line interface. Metashape is not the only COTS solution is this space. The ERDC team is continually monitoring progress in this community. An important point to note is that the framework developed using Metashape is a modular architecture where any component can be replaced/updated by open source or other COTS codes in the future.

The Metashape workflow follows a high-level process that is relatively standard throughout the SfM community. The process to generate 3D geospatial data from overlapping imagery uses these same four general steps:

- Feature Matching: The software automatically detects and identifies features within the imagery that are consistent through the different viewpoints. These in effect can be thought of as conjugate tie-points (or correspondences in SfM terminology) across the various images that are used with the photogrammetric process. While this image-to-image feature matching is all that is necessary to build a relative 3D model

using the additional steps outlined below the introduction of ground control is required to assess *true* geospatial accuracy and is very likely needed to assure acceptable co-registration to other geospatial data. An automated approach to bringing in the ground control is the focus of this work.

- Bundle Adjustment: Using an iterative approach based upon co-linearity, the interior (optical distortion and alignment) and exterior (position and orientation of the cameras) parameters of the camera system are adjusted. A number of methods that consider computational expense, weighting of parameters, and filtering of outliers are used in the community. However, after adjustment, the new camera positions and pose can be used to extract 3D structure from the features observed in the images. Typically, after bundle adjustment, a rough 3D representation of the features is generated. This is often called a Sparse Point Cloud.

- Dense Reconstruction: Once the camera calibration and refined position and pose of the cameras (during collection) have been computed, the task of determining a depth value (elevation) for each pixel pair is now possible. As with each of the preceding steps, a multitude of algorithms and techniques can be employed as part of the dense reconstruction process. Each of these techniques may be suitable for specific nuances associated with the camera types, collection patterns, objects of interest, or final output details (resolution, smoothness, noise reduction, etc.). The typical product after dense reconstruction is a point cloud that is many orders of magnitude larger (denser points, larger file size) than what is generated during the bundle adjustment / spare reconstruction process.

- Product Generation: A final step in the SfM pipeline is the generation of products that would be used for the needed application. These could include applications such as mapping, visualization, and mensuration. Standard products include colorized point clouds, digital terrain models, and orthometric mosaics. Other derived products may include interpolated surface models that could be rasterized to a standard grid or to a format that takes advantage of large planar areas such as triangular irregular networks. Other methods can include meshing and filling techniques such as Poisson surface filling and fitting of geometric primitives to the point clouds. During this step, algorithms

often are used to "texture" the planar surfaces with sections of the imagery, which produces a superior visual product than methods that interpolate colors from point vertices.

It is important to understand the difference between SfM and photogrammetry. In practice, the mathematics of the simultaneous bundle adjustment are often the same. However, the difference between the two is usually the rigor of the calibration and understanding of the uncertainties. Analytic photogrammetry "adheres to engineering principles such as geometric network design, metric camera considerations, accuracy optimization and variance propagation, systematic error compensation and gross error detection, scene-independent camera calibration, the adoption of observational redundancy to enhance reliability and quality control procedures at all stages of the photogrammetric data processing pipeline" (James 2019). While most SfM software has the capability to exploit this rigor, typically the SfM approach focuses on camera localization, and other parameters are left to be solved via the adjustment, which at numerical solution may or may not accurately represent reality (Schonberger 2016) (Schonberger et al. 2016).

2.2 Geo-registration to reference foundation

Each of the software packages selected for this study uses SfM and multi-view stereo algorithms that implement many standard photogrammetric concepts. While specific details are not provided by the vendors for competitive reasons, each package uses highly efficient central processing unit (CPU) / GPU computer vision techniques to generate large numbers of image match, or tie points. These tie points, which can be supplemented by ground control points (GCPs), are then used to generate an exterior orientation and interior/optical calibration using a bundle-block adjustment. After this second adjustment, the final geospatial products can then be developed.

The ERDC-GRL Auto-GCP algorithm utilizes computer vision techniques based on feature detectors and descriptors. David Lowe did foundational work with the development of the Scale Invariant Feature Transform (SIFT) method (Lowe 1999). The SIFT method is capable of performing matching between two images with different scales and orientations. Over the years additional techniques have been developed based on the original SIFT work. These methods include KAZE (a Japanese word for "wind") (Alcantarilla 2012) and Accelerated-KAZE (AKAZE) (Alcantarilla 2011).

For the Auto-GCP pipeline, the ERDC-GRL team adapted the AKAZE operator available within the Open-Source Computer Vision library (OpenCV) (Ruby and Massaro, in press). The AKAZE method uses what is known as a variable conductance diffusion approach to remove noise and retain image details for feature mapping. The AKAZE method also implements a fast explicit diffusion (FED) model within a pyramidal framework, which can dramatically improve performance over the original KAZE approach.

The overall ERDC-GRL approach to GCP detection is to identify and then match features between the image frames to be referenced and foundation data using the AKAZE algorithm. The feature detection step produces a large set of matching points, the vast majority of which are invalid matches. To filter the matches, the software looks for sets of points that fit a geometric transform between the two datasets. For the datasets described in this work, an affine model that allows for translation, rotation, and a change in scale and skew between the datasets was selected. If sufficient matches are found (typically more than 25), the match is assumed to be valid, and the pixel positions are converted to geographic coordinates.

While in this effort four sensors over four geographic regions were tested, this is hardly an exhaustive sample set. There are many factors that can affect the quality of the image matching step (between the sensor data to be registered and the foundation data), which impacts co-registration and geometric accuracy. Other factors include:

- Different sensor modalities (different spectral ranges)
- Large spatial resolution differences
- Large temporal changes (different seasons)
- Large illumination changes (sun angle, shadow)
- Orientation changes (look angle from sensor)
- Algorithmic settings in the AKAZE code
- Weighting of parameters in the bundle adjustment

In the cases examined for this work, a few of the factors included spatial resolution differences and temporal changes between the drone/FMV imagery and the reference data. Future investigations will examine some of the additional factors.

3 Reference Sources

3.1 GRiD

The Geospatial Repository and Data (GRiD) Management System was developed in partnership between the US Army Corps of Engineers Cold Regions Research and Engineering Laboratory (CREEL) and the National Geospatial-Intelligence Agency's (NGA) InnoVision Directorate to efficiently warehouse and distribute both 3D data, such as LIDAR, as well as related and derived 2D geospatial products, such as imagery and digital elevation models (DEMs). Originally focused on supporting LIDAR sensors that were fielded during Operation Enduring Freedom (OEF) and Operation Iraqi Freedom (OIF), GRiD has evolved into a repository for multiple domestic and international data sources to include those collected or purchased by USGS, NOAA, USACE and other federal agencies.

The UNCLASSIFIED version of GRiD is at https://grid.nga.mil/grid). Current data types stored include point-clouds, digital surface models (DSMs), bare-earth digital terrain models (vegetation and manmade objects removed), and orthometric image products.

GRiD allows for both a GUI and an application programming interface (API) approach to query, process, and download data products. An example is shown in the following two figures. Figure 1 is a Google Earth screenshot showing an area over Jalalabad, Afghanistan, that is used as part of the analysis in Section 4.2. The green line in Figure 1 shows the boundary of the data of the ARTEMIS drone that was flown over Jalalabad and was used as an input area of interest (AOI) to query within GRiD. Figure 2 shows the GRiD GUI with the search results from the AOI in Figure 1. In this example, GRiD was queried for digital surface models that covered that AOI. On the right-hand panel, two BuckEye LIDAR tiles have been selected. The green overlay on the image represents the area covered by the highlighted BuckEye tile in the right panel. These two DSM files were used as the foundation data in Section 4.2. A similar approach was followed for all processes where GRiD was used as a source for the foundation data.

Figure 1. Google Earth Pro location of the Jalalabad ARTEMIS data to be used for processing in the following section. The green box is 2.5 km × 1.5 km.

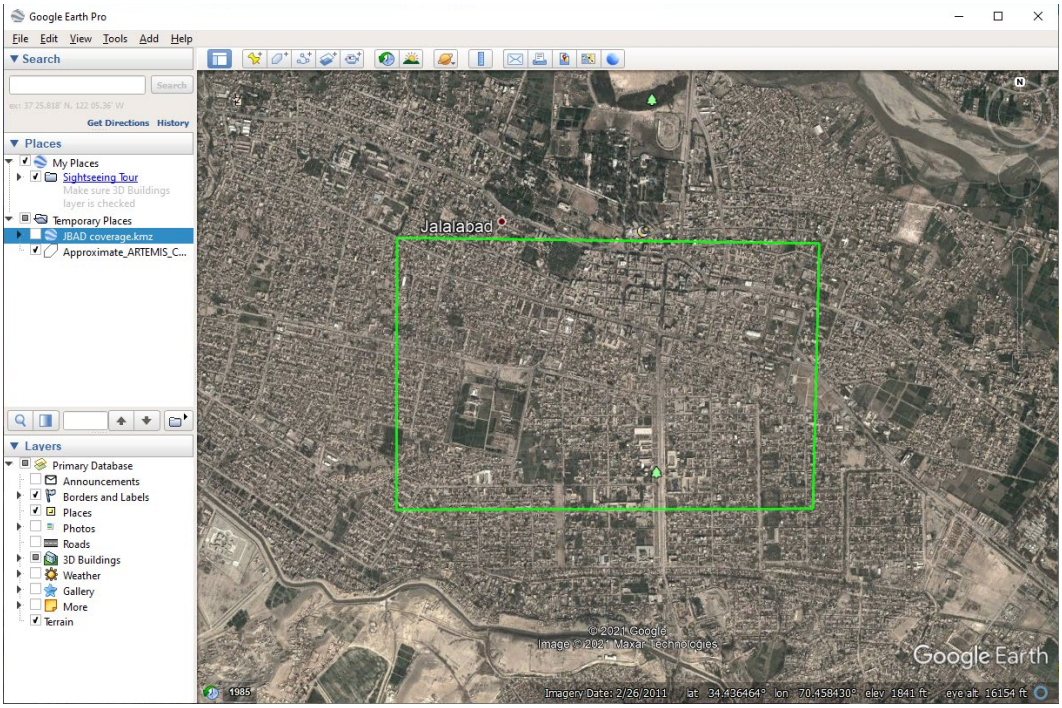

Figure 2. GRiD interface showing reference data available over the same area of Jalalabad, Afghanistan, from Figure 1.

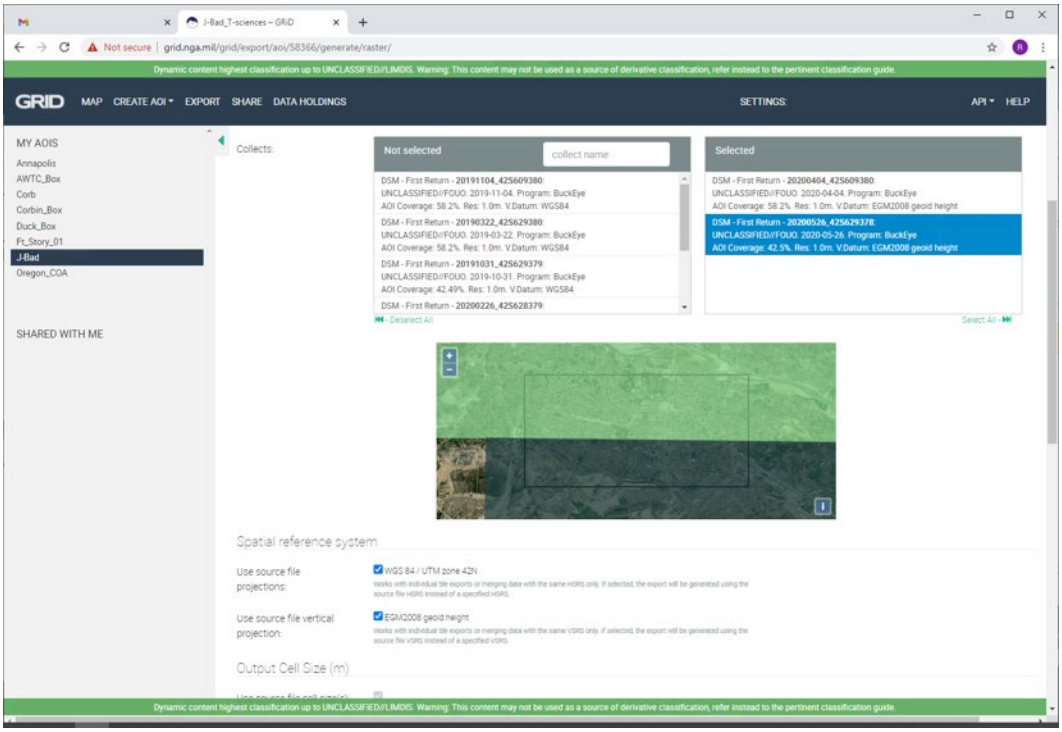

3.2 TAK-TICS

A second data source that has been used as foundation data by ERDC-GRL is the Tactical Assault Kit—Timely Imagery Content Services (TAK-TICS). TAK-TICS is a joint capability developed by NGA and the TAK Program Office to provide users with the ability to rapidly search, discover, view, and stream or download imagery and elevation data from commercial and tactical sensors. The primary objective is to provide this data directly to Windows TAK (WinTAK) and Android TAK (ATAK) end-user devices (EUD) but is exploitable by other government geospatial systems and programs. TAK-TICS is hosted on the unclassified Government Cloud and accessible through a web browser with a registered account. Geospatial data are constantly updated and stored in TAK native formats for ingestion onto TAK EUDs in both connected and disconnected environments.

TAK-TICS provides the user with the specific following capabilities:

- Search and discover near-real-time satellite and tactical imagery and elevation by designating an area of interest directly on a map.
- View image footprints and pixels on terrain. Removes the need to launch an external application to view imagery.
- Stream or download imagery directly into third party analytical tools, such as TAK, Google Earth, or ArcGIS Pro through OGC web-compliant services such as Web Map Service (WMS), Web Map Tile Service (WMTS), and Web Coverage Service (WCS), or download as native TAK tiles for use in disconnected environments. For larger requests, end users can request PIXIA Incorporated HiPER drivers.
- Access TAK-TICS through a thin-client web browser optimized for Chrome, Firefox, and Internet Explorer.

The procedure that has been used by ERDC-GRL to exploit reference data from TAK-TICS is slightly different than that used for GRiD. Where the GeoTIFF products from GRiD can be directly incorporated into the GRL processing pipeline, data from TAK-TICS requires some preprocessing. A common data format stored on TAK-TICS is Portable Reference Imagery (PRI) files. PRI are tiled image datasets corrected using Digital Terrain Elevation Data (DTED) or Shuttle Radar Topography Mission (SRTM) elevation data. GOTS code is available to perform this task. The ERDC-GRL team used the PRI Generator software built by the U.S. Naval Air Warfare Center (NAWC) and IAI, Inc. The PRI Generator can ingest

commercial satellite “Level 1B” imagery and DTED or SRTM. The PRI Generator then uses the rational polynomial coefficients (RPCs) of the Level 1B satellite image with the digital terrain data to accurately re-register the image data and outputs it into a National Imagery Transmission Format (NITF) file that includes the RPCs for geospatial referencing.

4 Results and Analysis

Each of the datasets analyzed in the following subsections were processed using the same basic geo-registration approach. This pipeline was developed by ERDC-GRL and integrates a mix of open-source, COTS, and GOTS utilities. The basic pipeline flow is shown in Figure 3 and described in detail below.

Figure 3. The ERDC-GRL automated-GCP processing pipeline. Input data are the FMV/Drone imagery in JPEG format, the reference/foundation imagery, and the reference/foundation elevation. Blue boxes represent geospatial data, while the green boxes are processing and analysis steps.

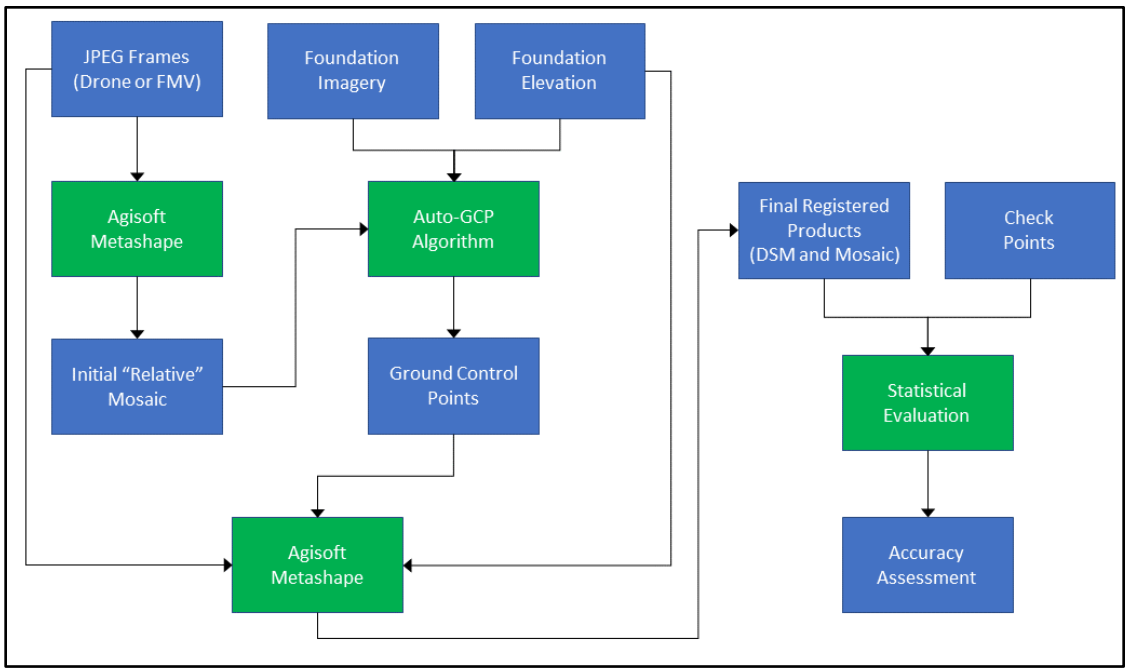

The initial step in the process is to acquire the imagery to be geo-registered (drone or FMV feed) as well as the foundation data. The drone or FMV data is converted to Joint Photographic Experts Group (JPEG) or Tagged Image File Format (TIFF) and combined with associated metadata that contain estimates for position and pose of the sensor during acquisition, the focal length and distortion parameters of the optics, as well as datum and projection information. This combined image and metadata is then processed by Agisoft Metashape to refine the position, pose, and distortion parameters through a self-calibrating bundle adjustment and generate what is sometimes called a "relative" mosaic (Steffen, Frahm, and Forstner 2010). In Figure 3, we refer to this product as the initial mosaic.

The next step uses code integrated at ERDC-GRL to perform feature-based image matching between the raw pixel data in the "relative" orthomosaic and the reference foundation data. This technique establishes matching pairs of *i,j* pixel values in the relative mosaic with geo-registered pixels in the reference foundation data (Figure 4). This produces a set of Ground Control Points (GCPs) that will exist and be detectable within the original JPEG files.

Figure 4. Flowchart breaking out the Auto-GCP Algorithm box shown in Figure 3. The Matching on Descriptors step uses a k-Nearest Neighbor (kNN) matching norm method, the Match Ratio Filter uses the Lowes Ratio Test (Lowe 1999). Blue boxes represent geospatial data, while the green boxes are processing and analysis steps.

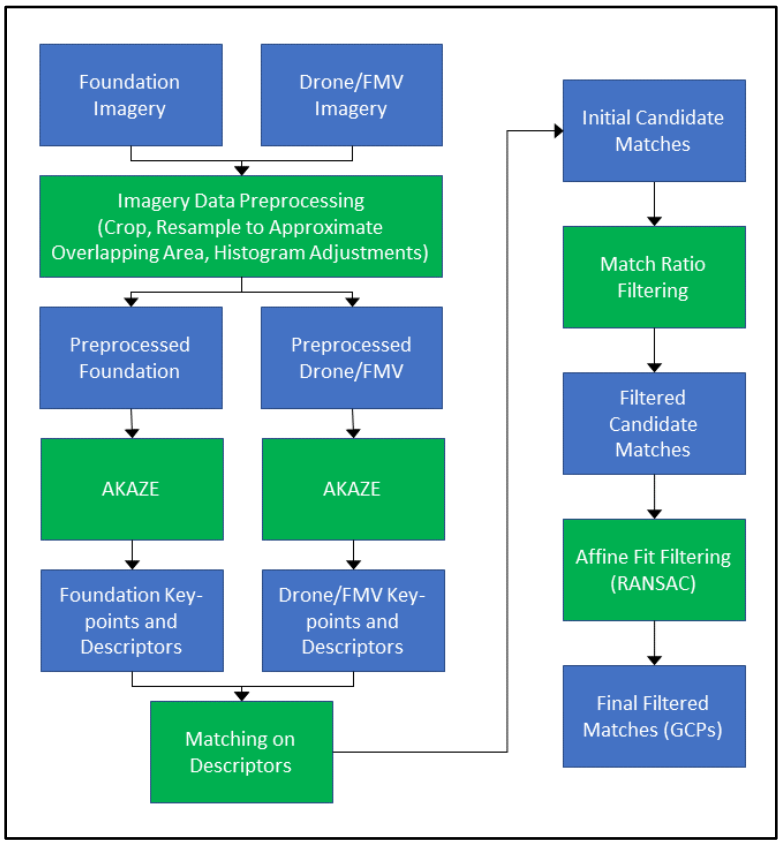

Agisoft Metashape is then used a second time to back-calculate the *i,j* pixels in the individual JPEG files based upon the now-"registered" *i,j* pixels in the relative mosaic. The bundle adjustment is run a second time using these GCPs, and Agisoft Metashape then produces geo-registered products to include a point cloud, DSM, and orthomosaic.

The final step is the statistical analysis to generate the accuracy assessment of the co-registration. Checkpoints that are photo-identifiable

in both the registered drone/FMV products and the foundation data are selected and measured. Ideally checkpoints will be located across the geographic extent of the region of interest with good relative spacing. COTS or open source software such as ArcGIS or QGIS are used to measure the absolute coordinates in both datasets. These measurements are then used to generate standard evaluation statistics as described in the US Army Corps of Engineers Photogrammetric and LiDAR Mapping Engineer Manual (US Army Corps of Engineers 2015) and the American Society of Photogrammetry and Remote Sensing (American Society of Photogrammetry and Remote Sensing 2015), shown below:

$$RMSE_x = \sqrt{\frac{\sum_{n=1}^{i}(Mx_i - Gx_i)^2}{n}}$$

$$RMSE_y = \sqrt{\frac{\sum_{n=1}^{i}(My_i - Gy_i)^2}{n}}$$

$$RMSE_z = \sqrt{\frac{\sum_{n=1}^{i}(Mz_i - Gz_i)^2}{n}}$$

$$RMSE_r = \sqrt{RMSE_x^2 + RMSE_y^2}$$

$$RMSE_{3D} = \sqrt{RMSE_x^2 + RMSE_y^2 + RMSE_z^2}$$

In this representation, *M* is the measured point from the drone/FMV data; *G* is the point measured from the foundation data; *x, y,* and *z* are the traditional cartesian coordinates (usually in UTM space); and *i* denotes the checkpoint measured. The *RMSE* statistics are the root mean squared errors in *x, y, z,* radial (*r*), and three dimensions (*3D*).

4.1 Fixed-wing sUAS, Corbin, VA (SmartPlanes Freya)

The first dataset selected for analysis was collected over the National Oceanographic and Atmospheric Administration (NOAA) Field Station in Corbin, VA. The Corbin site is located immediately to the north of Fort A. P. Hill, VA, and borders the middle-Atlantic coastal plane and middle-Atlantic Piedmont ecological zones. The site is approximately 0.32 km^2

and consists of forest, open grass areas, and a few small, one-story structures.

The drone used to collect the imagery was the Freya platform built by SmartPlanes LTD of Sweden. The Freya is used throughout Europe and Africa for surveying, mapping, mining, forestry, agriculture, and wildlife protection missions. The Freya drone is made of ruggedized foam, light plastic, and carbon fiber composites. The electric propulsion supports multiple battery and camera options. The flying parameters of the Freya platform for the Corbin collect are shown below:

- **System weight:** 1.1 kg
- **Wingspan:** 95 cm
- **Maximum flight time:** 75 minutes
- **Nominal cruise speed:** 40–60 km/hr
- **Radio range:** 15 km
- **Maximum wind usage:** 60 km/hr

The digital camera used with the Freya platform for the Corbin site was the Ricoh GRII.

The Ricoh GR camera family has a high-sensitivity, wide dynamic range Advanced Photo System type-C (APS-C) large-size complementary metal-oxide semiconductor (CMOS) sensor. The camera array is 16.2 megapixels and uses a fixed focal length of 18.3 mm. An interesting feature of the Freya platform is that the Ricoh GR camera is mounted with the long direction forward, which is useful for fast flying aircraft but the operator/flight planner must be aware of the reduced overlap between flight lines.

The specific parameters for the Ricoh GRII and a picture of the Freya drone and Ricoh GRII camera are shown below (Figure 5).

- **Camera:** Ricoh GRII
- **Nominal focal length:** 18.3 mm
- **Pixel array:** 4928 × 3264 (16.2 Megapixels)
- **Pixel size:** 4.8 μm
- **Spatial resolution as flown:** 3.5 cm

Figure 5. The SmartPlanes Freya and Ricoh GRII camera used for the Corbin data collection.

The Freya imagery obtained over the Corbin site was acquired on September 22, 2016. A total of 181 frames were collected via East–West flight lines. The flying height was about 130 m above terrain, which resulted in a nominal spatial resolution of 3.5 cm. The location of the Corbin site as well as the bounding box of the Freya imagery is shown in Figure 6. A close-up depiction of the bounding box and the exposure position of the 181 frames of the Freya images are shown in Figure 7.

Figure 6. Corbin location with boundary of the Freya flights from September 22, 2016.

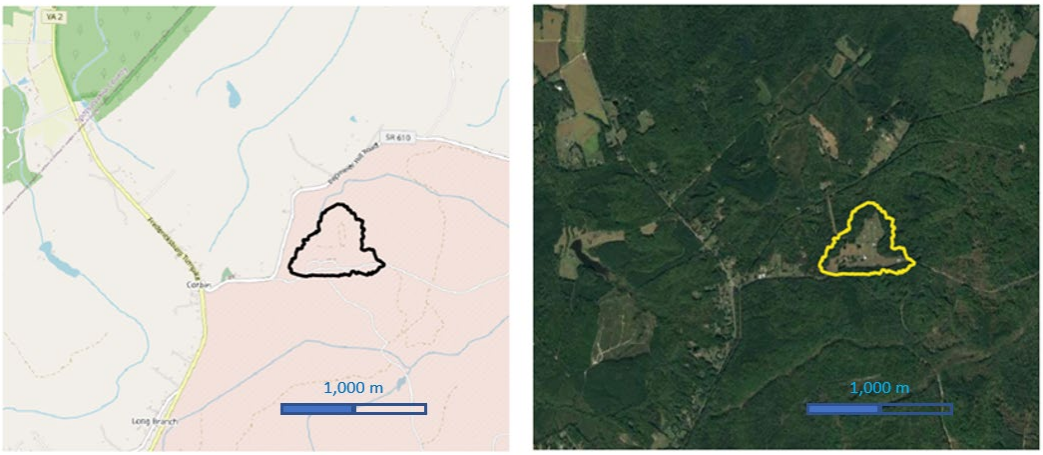

Figure 7. Bounding box of the Freya coverage (left) and the location of the individual Freya frames during collection (right).

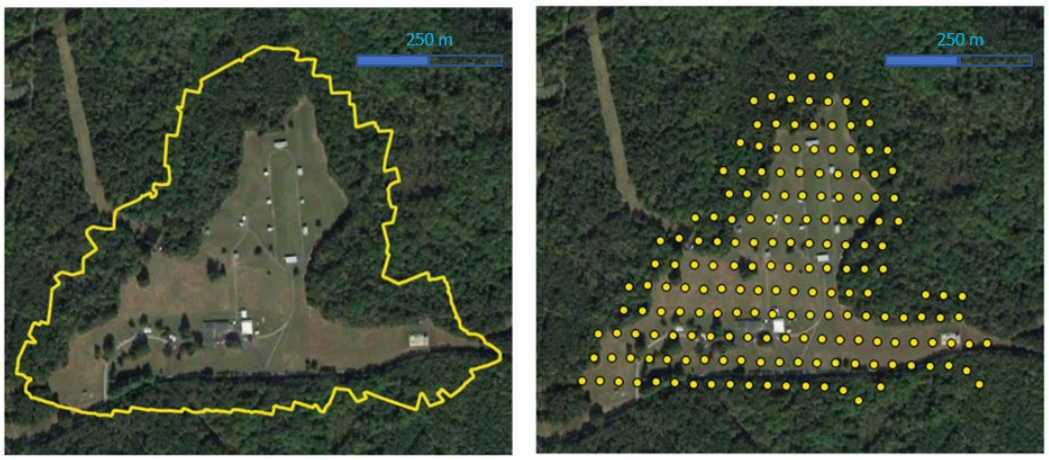

The Freya drone data over Corbin was initially processed using the SfM approach described in Section 2. BuckEye reference data from April 3, 2020, was obtained from both GRiD (as described in Section 3) and the GRL Auto-GCP pipeline (as described at the beginning of Section 4). The Corbin data were processed on a typical Windows 10-based desktop machine (Intel Pentium i7-7700 CPU, 32 GB RAM, NVIDIA GeForce GTX 1080 GPU), which took approximately 1 hour to complete the automated steps. Multiple Auto-GCP settings were used to assess the ability to extract GCPs within the Corbin environment. The total number of GCPs generated varied from 71 to 404 (shown in Table 1).

A sample of the output Freya product after completion of the initial mosaic (see Figure 3) compared to BuckEye is shown in Figure 8. Sample Auto-GCPs generated from the GRL pipeline are shown in Figure 9.

Figure 8. Freya drone (left) and BuckEye (right) orthomosaic outputs (right).

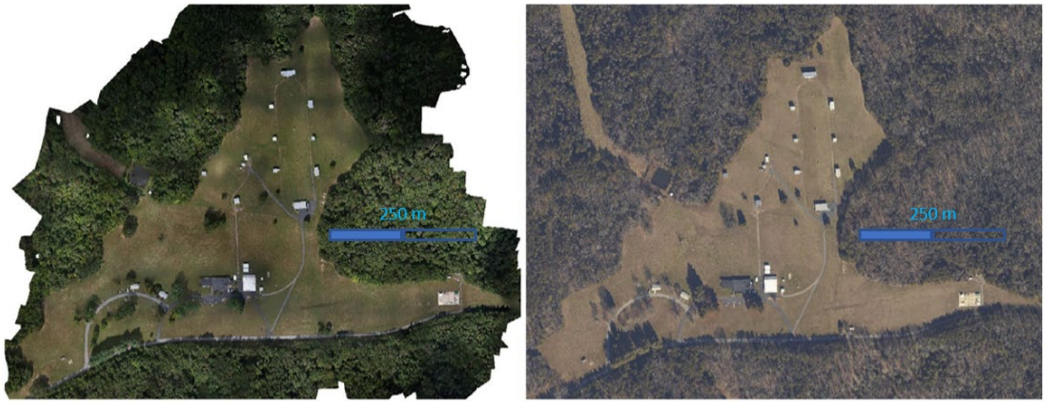

Figure 9. Sample automated GCPs generated by the GRL pipeline. Freya drone data are on the left, BuckEye reference data from GRiD are on the right.

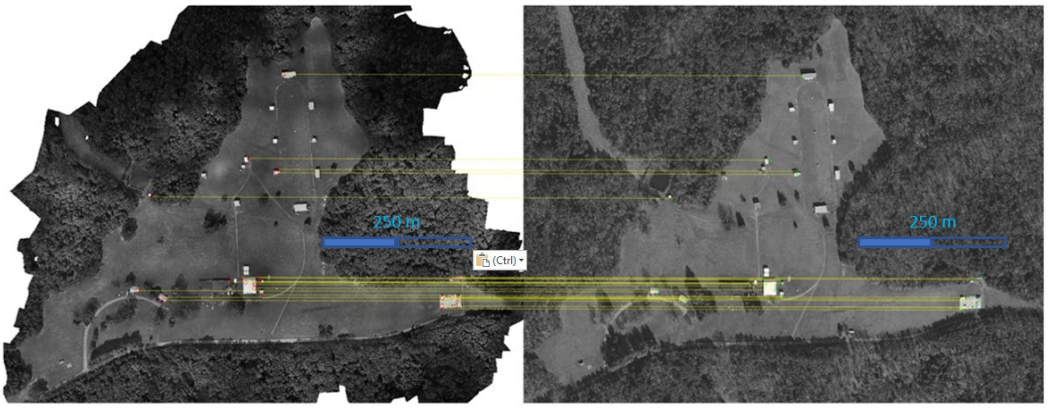

After bundle adjustment with the inclusion of the GCPs (second use of Agisoft Metashape in Figure 3), the co-registration of the output products was assessed using 19 checkpoints spread throughout the scene. These checkpoints are photo-identifiable features in both the Freya and BuckEye image products. Typically, these features can include natural and manmade objects that are measurable to the pixel level. Examples could be dashes and lines painted on asphalt, concrete edges, and specifically created/placed objects such as air photo targets. Ideally, these checkpoints will be located in areas without substantial vertical changes, which can introduce errors in height (z) due to slight offsets in the horizontal dimensions.

The spatial distribution of the checkpoints and a closeup of checkpoint #3 are shown in Figure 10.

Figure 10. Checkpoints used to assess co-registration accuracy between the Freya and BuckEye reference data. The spatial distribution is shown on the left side, while a detail of a painted target is shown on the right.

Four different sets of input parameters were tested during the Auto-GCP process to understand the impact of these parameters on performance for the Corbin environment. Two different settings for two parameters were varied. The first was the RANSAC Residual Threshold (RRT). The RRT is used during filtering of potential matches between the two data sets via estimation of a geometric transform between data sets. The RRT is the maximum allowable residual error between a given solution and a perfect geometric transform. As discussed above, an affine geometric transform is used to find the best set of matches between the two data sets. A low RRT value will have a "tight" affine fit, meaning the points will match an affine model closely. Higher RRT values will have a "loose" affine fit, and there will be more error in the solution compared to an ideal match. A tight fit is not necessarily better, as this could remove matches in certain "noisy" spatial regions such as near tree lines. Conversely, too loose of an RRT value could lead to the inclusion of pure blunders, which will negatively impact the overall co-registration accuracy. For the Corbin site data, RRT values of 1.5 and 6.0 were reported.

The second parameter varied was the tiling approach used on the low-accuracy orthomosaic during the matching process. As the memory usage and processing time during this step is proportional to the number of pixels in the corresponding mosaics, techniques to smartly reduce pixel

counts or break the mosaic files into sections can result in substantial time savings. The first approach was to resample the Freya drone initial mosaic to 3,000 pixels in the largest dimension. This is called "Quick" processing in the ERDC-GRL Pipeline. This resulted in a nominal working spatial resolution of 23 cm. The second approach was to break the Freya initial mosaic into multiple 3,000 × 3,000 pixel tiles at a spatial resolution equal to the reference data resolution. This method resulted in a working spatial resolution of 10 cm. This is called the "Tiles" approach (Figure 11).

Figure 11. Depiction of Quick versus Tiled processing approaches. The left side shows the Quick approach for the Corbin data set. The yellow box has been resampled into a single tile with 3,000 pixels in the long (horizontal) direction. The right side shows the Tiled approach, the larger boxes are 3,000 × 3,000 pixels, while smaller, "remainder" boxes are shown on the bottom and right edge.

From a performance perspective, the Quick processing approach is faster than the Tiled approach. However, in either case, for a dataset this size (181 frames), the Auto-GCP step was only a small percentage of the total processing time. (1.5 minutes for Quick and between 4 and 4.5 minutes for Tiled, out of the total of about 1 hour). With the coarser working spatial resolution, the Quick approach can address larger horizontal offsets between the initial drone mosaic and the reference data. While slower, the Tiled approach will generate more GCPs and at the native spatial resolution, which in theory would be more accurate via the better precision of the pixel matching.

The statistical assessment of the four processing variants is shown in Table 1 below.

Table 1. Co-registration statistics between Freya drone data over Corbin and the BuckEye reference data.

Processing Type	Working Resolution (m)	Number of Auto-GCPS	Root Mean Square Error (m)				
			x	*y*	*z*	2D	3D
EO Quick, RRT 6.0	0.23	279	0.33	0.24	0.07	0.38	0.39
EO Quick, RRT 1.5	0.23	71	0.33	0.18	0.06	0.37	0.37
EO Tiles, RRT 6.0	0.10	404	0.32	0.16	0.07	0.34	0.34
EO Tiles, RRT 1.5	0.10	98	0.29	0.31	0.08	0.42	0.43

As expected, the RRT runs of 6.0 generated a much larger number of GCPs than the RRT 1.5 versions. The Tiled runs produced slightly more GCPs than the Quick runs. From the co-registration perspective, all methods produced very good results, with the 3D RMSE between 34 cm and 43 cm, which easily surpassed the 1 m threshold objective. The best result was the combination of an RRT of 6.0 using the Tiled approach. This makes intuitive sense as the larger RRT will detect more GCPs, especially boundary areas, and the Tiled method has a better pixel precision. However, when considering the time difference between the Quick and Tiled approach, the small co-registration deltas may be of secondary importance to processing speed. This would especially be true for large-area, time-sensitive applications, which would include many tactical missions. This trade between accuracy and processing time for the Quick versus Tiled approaches warrants further study.

4.2 Fixed-wing sUAS, Jalalabad, Afghanistan (senseFly eBee)

Since 2018, NGA has supported a seed initiative to provide an sUAS-based intelligence collection capability. Sponsored by the Warfighter Support Office within NGA, the Aerial Reconnaissance Tactical Edge Mapping Imagery System (ARTEMIS) program has fielded over 30 sUAS kits to US military personnel across the globe. The objective of the ARTEMIS program is to allow local commanders to collect, process, disseminate, and exploit high-resolution 3D geospatial products of their area of responsibility.

ARTEMIS provides a crucial capability in areas where geospatial data are dated or too coarse of resolution to meet intelligence and reconnaissance requirements. This is often the case in areas that have been underserved by National Sensors in the past (such as Africa and the Pacific Rim region). Data collected from the ARTEMIS platforms contribute to understanding

the initial operating environment. ARTEMIS data are Unclassified, allowing the products to be shared with coalition and host nation partners.

ARTEMIS comprises several COTS components, which reduces complexity and cost. These components include a non-ITAR restructured surveying/mapping drone; high-resolution imagery sensors; collection software; Google Earth Enterprise Platform software; and a ruggedized, high-performance laptop computer. The ARTEMIS kits come with two aircraft, each with a standard EO camera, 3D EO camera, EO/IR camera, and low-light EO camera.

The ARTEMIS program currently uses the senseFly eBee sUAS (based in Geneva, Switzerland). The eBee is a small, fixed-wing, commercially available UAS platform commonly used within the drone mapping community for photogrammetric processing. The low cost and ease of replacement of eBee components was a major factor in NGA selecting the eBee for the ARTEMIS program. Details on the eBee are listed below. A version of the eBee platform is shown in Figure 12.

- **System weight:** 0.70 kg
- **Wingspan:** 96 cm
- **Maximum flight time:** 50 minutes
- **Nominal cruise speed:** 40–90 km/hr
- **Radio range:** 3 km
- **Maximum wind usage:** 45 km/hr

Figure 12. Sensfly eBee Plus. The coffee cup in the left image gives a representation of the size/scale of the eBee Plus drone.

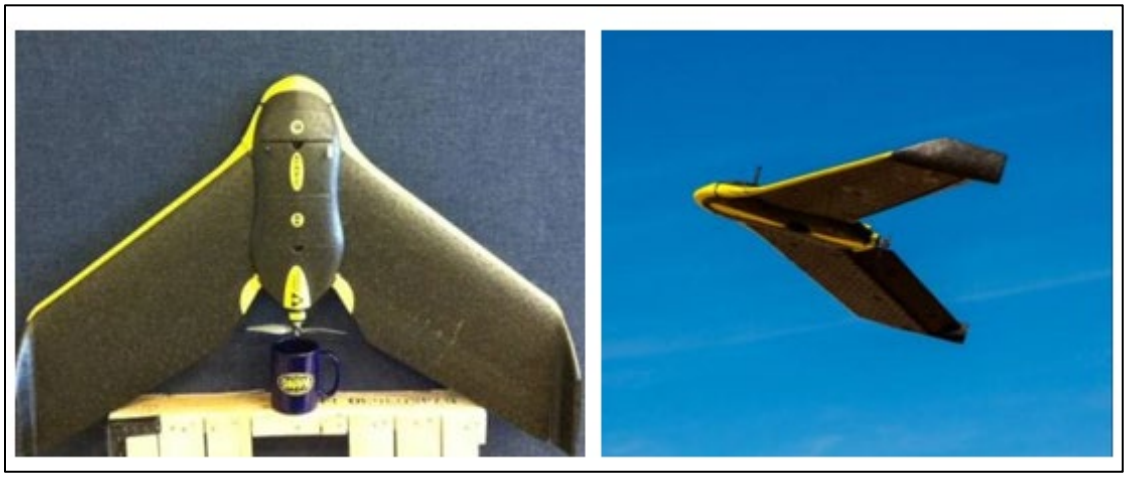

The specific ARTEMIS data used for this effort were collected over Jalalabad, Afghanistan, over three separate dates (six individual flights) in August 2020. The sensor used for this collection was the senseFly S.O.D.A camera, which is the first model developed specifically for the eBee platform. Details on the S. O. D. A. sensor are shown below.

- **Camera:** senseFly S. O. D. A
- **Nominal focal length:** 10.6 mm
- **Pixel array:** 5472 × 3648 (20 megapixels)
- **Pixel size:** 2.33 µm
- **Spatial resolution as flown:** 3.3 cm

The area covered by the ARTEMIS flights encompasses about 4.4 km² of the eastern part of Jalalabad on the south side of the Kabul River (Figure 13). Due to the large area of coverage, location of takeoff and landing points, and prevailing winds, the six flight lines had different lengths and directions. A total of 2,905 frames from 94 flight lines were collected over the three days. Camera settings and flying parameters from the Jalalabad ARTEMIS data are in Table 2. A schematic showing the flight lines and individual frames are on the right-hand side of Figure 14.

Figure 13. Location and area of coverage for the ARTEMIS flights over Jalalabad, Afghanistan.

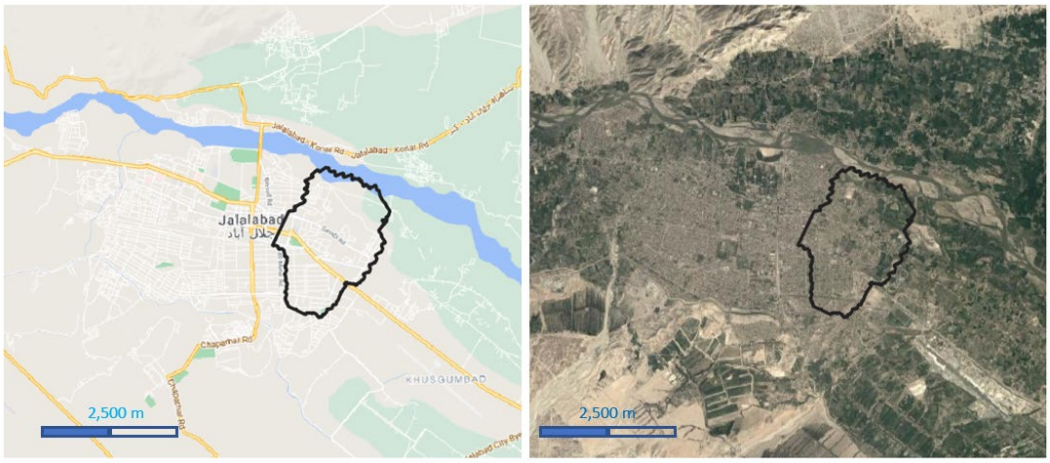

Figure 14. Area of coverage (left) and patterns for the individual flights that compromised the Jalalabad ARTEMIS data (right).

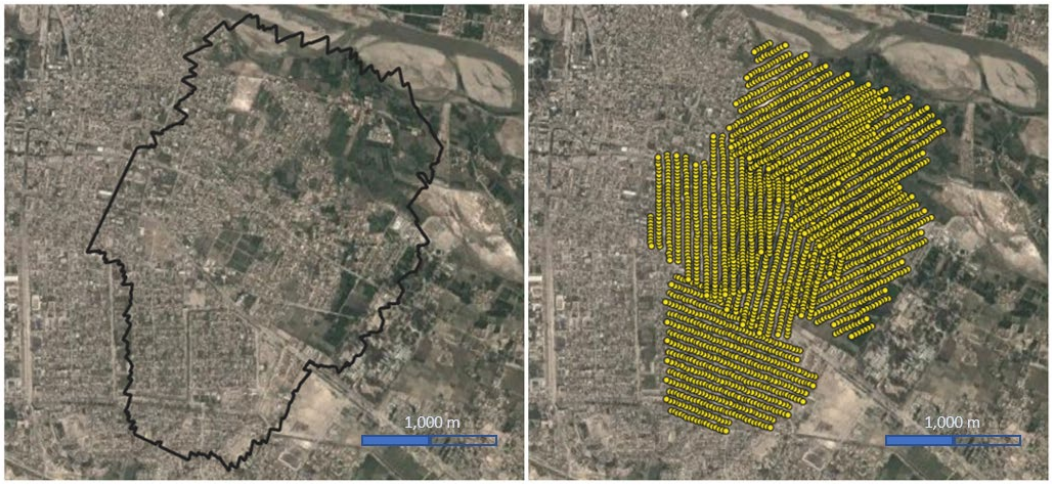

Table 2. Jalalabad ARTEMIS collection flight details.

Date (Lift#)	F-stop	Shutter (sec)	ISO	Flying Height (m)	Flight Direction	# Images
08/11/19 (32)	2.8–4.5	1/1000	125–250	150	NE/SW	504
08/16/19 (20)	2.8	1/1000	125–400	150	NE/SW	494
08/16/19 (21)	2.8–4.5	1/1000	125–400	150	N/S	446
08/23/19 (25)	2.8	1/1000	200–500	150	NNE/SSW	526
08/23/19 (26)	2.8–4.5	1/1000	125–160	150	NE/SW	512
08/23/29 (27)	2.8–3.5	1/2000–1/640	125	150	NW/SE	423

The Jalalabad ARTEMIS data were processed using the steps and hardware outlined in the previous sections. The reference data used for GCP generation was BuckEye from June 2018 downloaded via GRiD. As this site is substantially larger than the Corbin area, total processing time was considerably longer at approximately 25 hours.

Figure 15 shows a sample comparison between the BuckEye EO imagery at 10 cm spatial resolution and the ARTEMIS data at 3.3 cm spatial resolution. Both data sets are excellent, although with the ARTEMIS imagery it is possible to resolve the individual shingles on the tower of the UN building as well as more details on the satellite dish and roof. Also, it should be noted that the data depicted in Figure 15 is after the imagery had been resampled via the orthorectification process, so some aliasing is visible, particularly with the ARTEMIS data.

Figure 15. Visual comparison between BuckEye foundation imagery (left) and an individual ARTEMIS/eBee (right) image over a single building in Jalalabad, Afghanistan. The individual shingles and roof texture is visible within the higher spatial resolution ARTEMIS data on the right side.

Figure 16 shows the same building depicted in Figure 15 except that this is the DSM. Here the spatial resolution is substantially different. The processed resolution of the BuckEye DSM is 1 m, while the ARTEMIS DSM is at 13 cm resolution. A quick analysis also shows the obvious difference in the sensor modality that collected the data. The BuckEye DSM was created from a traditional pulsed LIDAR sensor. These LIDAR sensors transmit laser light from the aircraft to the ground in almost a nadir geometry, which works well in urban environments for reconstructing the vertical features of buildings and alleyways even though the spacing is relatively course. On the other hand, the photogrammetric reconstruction process can resolve smaller features but often introduces rounding or blurring of sharp edges. Geometric primitive fitting techniques such as those developed by the Intelligence Advanced Research Projects Activity Creation of Operationally Realistic 3D Environment program (IARPA CORE3D) are under evaluation for future integration into the GRL pipeline.

Figure 16. Comparison between ARTEMIS (left) and BuckEye (right) Digital Surface Models (DSMs). Color represents elevation in meters above the ellipsoid.

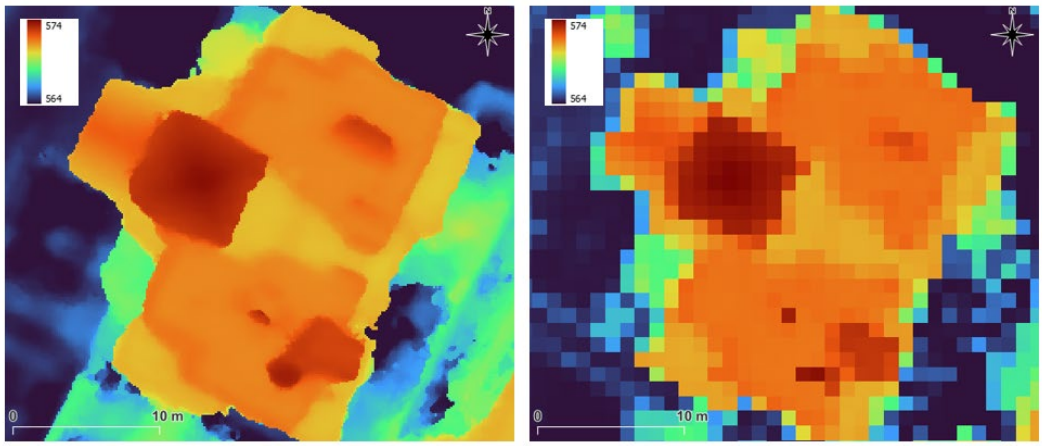

After initial processing and creation of the initial ARTEMIS mosaic (see Figure 3), the Auto-GCP software was used to find co-registration GCPs between the ARTEMIS data and BuckEye. The RRT parameter was set to 1.5, and both the Quick and Tiled methods were used. A total of 446 points were found with the Quick approach, and 1,098 points were found for the Tiled approach. These GCPs were then used as ground control to process the ARTEMIS data into the final products to be evaluated for co-registration accuracy assessment.

A total of 29 checkpoints were selected throughout the ARTEMIS Jalalabad coverage for evaluation. Figure 17 shows the location of the 29 checkpoints with a sample close-up of checkpoint 13. The checkpoints were selected in areas away from vertical surfaces to minimize DSM "rounding," as shown in Figure 16.

Figure 17. Location of the 29 checkpoints (left) used to evaluate the co-registration between the BuckEye data and the ARTEMIS products. The right side shows CP13 in the BuckEye orthomosaic.

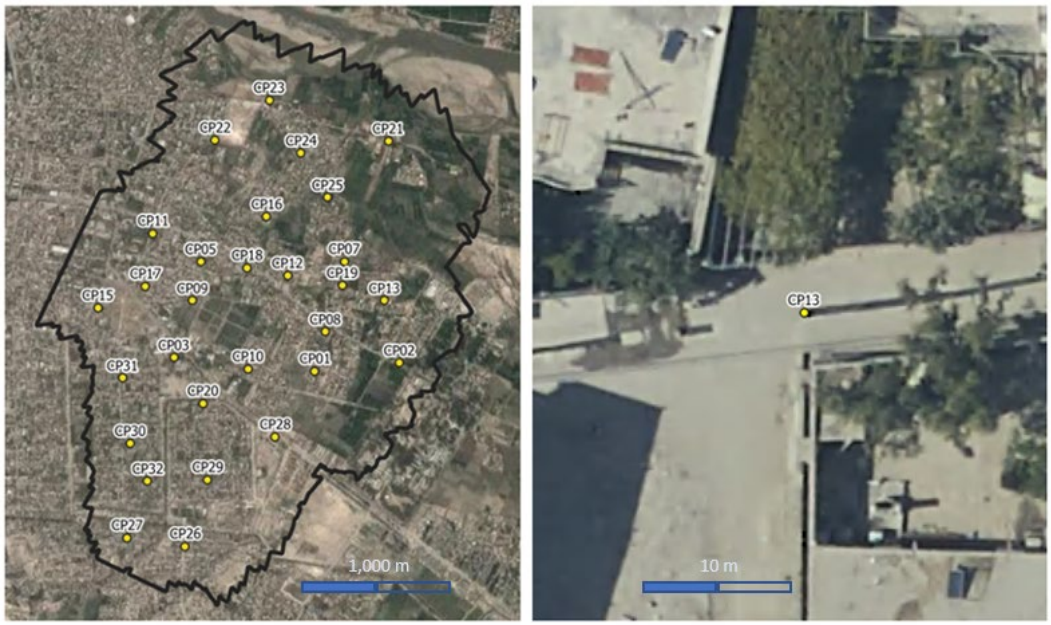

Table 3 shows the co-registration accuracy assessment for the 29 checkpoints. As with the Freya data over Corbin, the co-registration between the ARTEMIS data and BuckEye reference data is excellent. Results between the Quick and Tiled approaches were very similar. The 3D RMSE was 0.71 m for the Quick method and 0.75 m for the Tiled method, both of which are better than the 1.0 m objective threshold. However, processing time between the Quick and Tiled methods was substantially different. The generation of Auto-GCPs for the Quick method took approximately 10 minutes. The generation of Auto-GCPs for the Tiled method was over 1 hour and 15 minutes. While the 1 hour and 15 minutes Auto-GCP step for the Tiled approach could be considered a minor contributor to an overall processing time of 13 hours, it is still significant compared to the 10 minutes for the Quick method.

Table 3. Co-registration statistics between the Jalalabad ARTEMIS data and BuckEye reference data.

Processing Type	Working Resolution (m)	Number of Auto-GCPS	Root Mean Square Error (m)				
			x	*y*	*z*	2D	3D
EO Quick	0.79	446	0.36	0.41	0.45	0.55	0.71
EO Tiles	0.10	1098	0.30	0.41	0.56	0.50	0.75

4.3 FMV RQ-20, Puma, Camp Roberts, CA

The next dataset selected for analysis was an FMV feed from Camp Roberts, CA, collected by an RQ-20 Puma UAV. The RQ-20 Puma is a small, battery-powered, hand-launched unmanned aircraft system produced by AeroVironment based in California. The primary mission of the Puma is tactical surveillance and intelligence gathering through the electro-optical and infrared cameras on the sensor payload. Over 1,000 Puma aircraft have been built and deployed with the US Army, Air Force, and Marines and multiple foreign military partners.

Operating parameters of the Puma are shown below. A typical Puma aircraft in flight in shown in Figure 18.

- **System weight:** 6.3 kg
- **Wingspan:** 2.8 m
- **Length:** 1.4 m
- **Maximum flight time:** 3+ hours
- **Nominal cruise speed:** 50–90 km/hr
- **Typical operating altitude:** 500 m above ground
- **Radio range:** 20 km

Figure 18. RQ-20 Puma aircraft in flight without sensor payload.

The sensor payload for the Camp Roberts data was the AeroVironment Mantis i45. The Mantis i45 lightweight, compact, gimballed sensor allows for full hemispherical coverage below the aircraft. The systems includes EO, low light, and thermal options. The EO systems can operate in a 15 megapixel still mode as well as stream video. For the Camp Roberts collect, the sensor was in the streaming video mode. Parameters for the Mantis i45 follow. The Mantis i45 sensor is shown in Figure 19.

- **Sensor type:** Progressive scan
- **Resolution:** 480i/720i SD
- **Field of view:** 56° to 1.2°
- **Zoom ratio:** 50×
- **Dimensions (Diameter):** 11 cm
- **Weight:** 0.85 kg
- **Operating temperature:** –20 C to 50°C

Figure 19. Mantis i45 sensor used on the Puma RQ-20 aircraft.

Camp Roberts is located in the rolling hills just north of Paso Robles, CA. The site collected by the Puma UAS is a small training area located on top of a hill. Arid grasslands, dirt roads, and a few buildings make up the site. The area covered by the FMV data only covered about 0.13 km^2. The data were collected at an altitude of 350 m in a full orbit on February 19, 2020. Base data are VRICON point cloud data collected January 27, 2020. A total of 84 frames were extracted from the FMV feed to process through

the GRL pipeline. The functional spatial resolution of the FMV data was approximately 35 cm.

The location of the Camp Roberts data is shown in Figure 20, and an overview of the individual frames after initial registration (during low accuracy mosaic creation) is shown in Figure 21.

Figure 20. Location and coverage of the Camp Roberts Puma FMV data.

Figure 21. Puma FMV data coverage over Camp Roberts (left). The individual frames of the Puma FMV feed after photogrammetric adjustment within the Agisoft Metashape software (right).

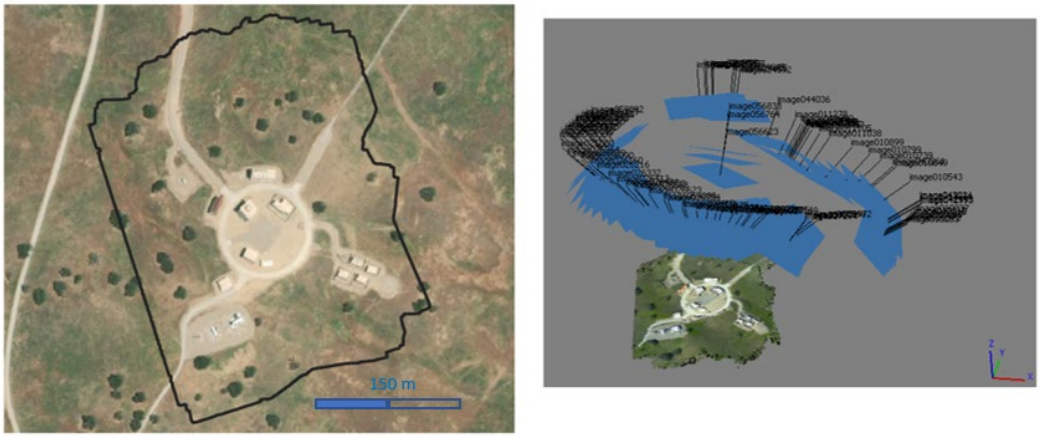

The reference data used within the Auto-GCP software was VRICON collected over the site in January 2020 and provided by NGA. Only the point-cloud data were downloaded; the DSM and image overlay were created from the point-cloud using the QT Modeler software package. The spatial resolution of the VRICON DSM and orthomosaic used within the Auto-GCP software was 50 cm.

The RRT for Camp Roberts was set to 3.0, and the Quick processing model was used. The RRT was slightly higher than the 1.5 in the previous section as it was observed that the initial mosaic misaligned by at least 10 meters, so a larger RRT was merited. The Quick processing approach was used as the size of the initial mosaic was less than 3,000 pixels and there was no need to tile the data.

Total processing time through the GRL pipeline was 7 minutes and 34 seconds. The total number of GCPs generated was 101 in 36 seconds. Figure 22 below shows an overview of the results. The left side of the figure is the VRICON data alone, and the right side shows the merged Puma/VRICON data after co-registration using the GRL pipeline.

Figure 22. VRICON Data over Camp Roberts (left).Merged VRICON and Puma FMV data after registration (right).

To assess co-registration accuracy, 10 checkpoints were identified around the “traffic circle” shown in the imagery. The checkpoints consisted entirely of intersection points between the concrete and dirt roads. The checkpoint distribution and a close-up view of two of the points (in the VRICON data) are shown in Figure 23.

Figure 23. Check point distribution from the Camp Roberts FMV data (left). Close-up of check points 001 and 002 on the pavement/dirt intersection.

Co-registration accuracy assessment between the Puma FMV data and the VRICON after processing is shown in Table 4 below. As with the Corbin and Jalalabad sites, the co-registration was excellent. The 3D RMSE was 0.49 m, which again is better than the threshold objective of 1.0.

Table 4. Co-registration statistics between the PUMA FMV data over Camp Roberts and VRICON reference data.

Processing Type	Working Resolution (m)	Number of Auto-GCPS	Root Mean Square Error (m)				
			x	*y*	*z*	2D	3D
EO Quick	0.35	101	0.17	0.32	0.33	0.37	0.49

4.4 FMV FLIR SS380, Cape Henry, VA

The fourth dataset processed for this effort was an FMV feed from a FLIR Star Sapphire 380 (SS380) High-Definition (HD) Sensor collected over Cape Henry, VA, on May 15, 2015. The type of aircraft used for this collect is unknown but was likely a manned, fixed-wing platform.

The FLIR SS380 system is typically used for missions that highlight the mid-wave infrared sensor (MWIR) but has options for a color HD, low-light color HD, and a short-wave infrared (SWIR) sensor. For the Cape Henry collect, the color HD feed was used. The SS380 is shown in Figure 24, while the pertinent specifications for FLIR SS380 Color HD Sensor are below.

- **Sensor type:** Progressive scan
- **Resolution:** 720p/1080p HD
- **Field of view:** 29° to 0.25°
- **Zoom ratio:** 120×
- **Dimensions (diameter × height):** 38.0 cm × 47.5 cm
- **Weight:** 45.4 kg
- **Operating Temperature:** −40°C to 55°C

Figure 24. FLIR Star Sapphire 380 HD Sensor (FLIR SS380HD).

The Cape Henry site is located near Virginia Beach, VA, and borders the Chesapeake Bay to the north and the Atlantic Ocean to the east. The environment is a mix of maritime forest, grassy dunes, soft and hard beaches, and built-up infrastructure to include two lighthouses.

The FMV feed used for this effort was collected on May 15, 2015, and consists of three 360-degree orbits over the site. The first two orbits are EO-Narrow (EON) collects over the two signature light houses on the site. The third feed, which was used for this effort, is an EO-Wide (EOW) collect that encompasses both lighthouses and the surrounding area. The location of the Cape Henry site with an outline of the EOW area of coverage is shown in Figure 25. A sample frame from the FMV feed is shown in Figure 26. The left side of Figure 27 shows the FMV coverage over the BuckEye orthomosaic, and the right side of Figure 27 shows the individual FMV frame positions after initial photogrammetric adjustment.

Figure 25. Location and coverage of the Star Sapphire Cape Henry FMV data.

Figure 26. Single Star Sapphire FMV frame from the lighthouse area of Cape Henry.

Figure 27. Star Sapphire FMV data coverage over Cape Henry (left). The individual frames of the Star Sapphire FMV feed after photogrammetric adjustment within the Agisoft Metashape software.

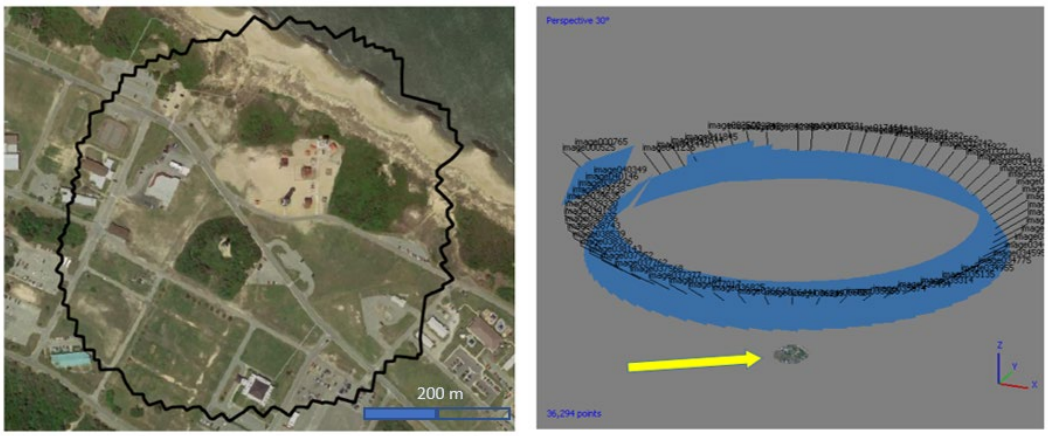

The BuckEye data used as reference was were collected in August 2015 and obtained from GRiD. A total of 65 frames from the EOW Cape Henry FMV feed covering about 0.25 km² were processed as described in the previous sections to generate the initial mosaic. Unlike the Puma data from Camp Roberts that was collected at a relatively low altitude (<500 m), the SS380 data was collected at approximately 2,650 m, which is typical for larger aircraft and systems.

For the Auto-GCP processing, the RRT for the Cape Henry data was set to 1.5, and the Quick processing model was used. Unlike the Camp Roberts data, the initial alignment between the BuckEye reference data and the initial mosaic was only a few meters. As with the Puma, the FLIR SS380 low accuracy mosaic was less than 3,000 pixels in the longest dimension, so the Quick processing approach was selected.

Total processing time through the GRL pipeline was 12 minutes and 46 seconds. The total number of GCPs generated was 848 in 1 minute and 21 seconds. Figure 28 shows an overview of the results. The left side of the figure is the BuckEye data alone, and the right side shows the merged SS380/BuckEye data after co-registration using the GRL pipeline.

Figure 28. Cape Henry BuckEye data (left) and Star Sapphire 380 FMV data (right) after co-registration to the Buckeye foundation.

To assess co-registration accuracy, 19 checkpoints were identified throughout the site. The checkpoints consisted of road intersections, painted lines, and utility hole covers. The check point distribution and a close-up view of checkpoint 8 (in both the BuckEye and FMV feed) are shown in Figure 29.

Figure 29. Checkpoint location and samples from Cape Henry (left). Upper right is checkpoint 8 from the BuckEye mosaic. Lower right is the same point shown in an FMV frame.

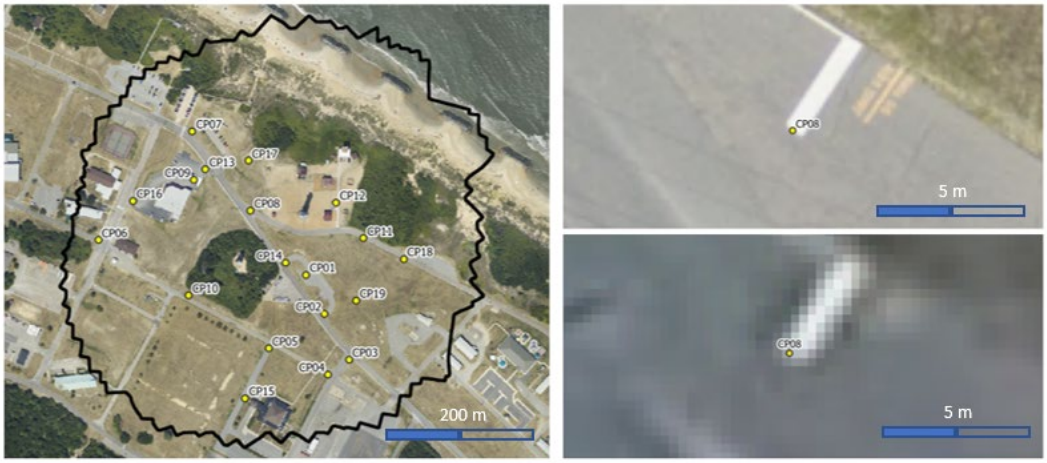

Co-registration accuracy assessment between the SS380 FMV data and the BuckEye data after processing is shown in Table 5 below. The co-registration between the datasets was the best of the four sensors and sites studied. The 3D RMSE was 0.37 m, which again is substantially better than the threshold objective of 1.0.

Table 5. Co-registration statistics between the FLIR FMV data over Cape Henry and BuckEye reference data.

Processing Type	Working Resolution (m)	Number of Auto-GCPS	Root Mean Square Error (m)				
			x	*y*	*z*	2D	3D
EO Quick	0.27	848	0.22	0.28	0.07	0.36	0.37

5 Discussion

Table 6 summarizes the results from all four sensors and terrain types across the various settings. The primary objective of this work was to demonstrate that the ERDC-GRL Auto-GCP pipeline could meet the objective threshold of 1.0 m co-registration between the tactical drone/FMV data and foundation sources. In all cases, both the 2D and 3D RMSE co-registration error is better than 1.0 m, with 3D co-registration accuracy ranging from result from 0.34 m (Corbin Freya Drone) to 0.75 m (Jalalabad eBee). Again, it is important to stress that the co-registration reported is not absolute accuracy (comparison to independently measured points through traditional means). However, co-registration is often more important for tactical visualization and mission rehearsal applications. For these uses, producing a seamless data product across sensor modalities and collection dates is critical for cognitive interpretation as well as exploitation through advanced analytical methods.

Table 6. Summary of results from all sensors, environments, and settings presented in Section 4.0.

Site and Sensor	Processing Type	GCP Working Res. (m)	Number of Auto-GCPS	Area (km^2)	Co-registration RMSE (m)		Processing Time (hr:min:sec)	
					2D	3D	CGPs	Total
Corbin Freya	Quick, RRT 6.0	0.23	279	0.32	0.38	0.39	00:01:38	01:00:32
Corbin Freya	Quick, RRT 1.5	0.23	71	0.32	0.37	0.37	00:01:44	01:00:06
Corbin Freya	Tiled, RRT 6.0	0.10	404	0.32	0.34	0.34	00:04:31	01:04:21
Corbin Freya	Tiled, RRT 1.5	0.10	98	0.32	0.42	0.43	00:04:04	01:02:42
Jalalabad eBee	Quick, RRT 1.5	0.79	446	4.4	0.55	0.75	00:09:21	24:49:57
Jalalabad eBee	Tiled, RRT 1.5	0.10	1098	4.4	0.50	0.75	01:18:00	25:58:36
Camp Roberts Mantis i45	Quick, RRT 1.5	0.35	101	0.13	0.37	0.49	00:00:36	00:07:34
Cape Henry SS380 HD	Quick, RRT 1.5	0.27	848	0.25	0.36	0.37	00:01:21	00:12:46

Further analysis of Table 6 shows additional interesting information. First, for the two drone data sets that covered larger areas (the Freya over Corbin

and the eBee over Jalalabad), the co-registration *RMSE* appears to be independent for the settings used, especially the Quick vs. Tiled method. What is important is the time difference for the Auto-GCP step. While the GCP generation time difference between the two methods for the Freya data are relatively small (1:44 min vs. 4:04 min for the RRT = 1.5), that is not the case for the Jalalabad set. Here the time difference is substantial, 9:21 min for the Quick method and 1:18:00 hr for the Tiled approach. In most cases, the GCP generation step took approximately 5% of the total processing time. The only outlier was the SS380 HD data over Cape Henry, which were close to 10% (but generated 848 GCPs). As noted in Section 4.2, for time-sensitive tactical situations, the Quick processing would be the preferred method. The time difference is correlated most closely with the working GCP resolution, where the ratio between the working GCP resolution is roughly the same as the ratio of processing times between the Quick/Tiled methods. Further analysis is necessary to see if this roughly linear relationship holds.

A second component to GCP generation for further evaluation is the how the number and spatial extent of the GCPs impact co-registration. Analysis of Table 6 shows that neither the processing time nor the co-registration accuracy is dependent on the number of GCPs generated. Typically, feature-matching codes such as AKAZE detect many points that are close in proximity. These highly correlated clumps of points do little to improve overall co-registration, as they can be clustered in only a few of the overlapping frames. An approach that generates even larger numbers of GCPs (that doesn't significantly impact processing time) but with advanced filtering to ensure adequate spatial distribution and blunder removal (such as GCPs within erroneous zones) would be beneficial.

Associated with the co-registration assessment is the need to study in more detail areas that have substantial changes in elevation. All checkpoints across the four datasets used in this study were measured from areas that were at ground elevation and away from vertical changes. As noted in Section 4.2, the SfM-generated DSMs for Jalalabad were "rounded" in comparison to LIDAR-generated models. A follow-on analysis where checkpoints were selected from tops of buildings, especially in modern urban areas, would verify that the methods used in this effort were universal in their applicability.

Beyond the two parameters varied in the Auto-GCP approach (RRT and Quick vs. Tiled), there are many other settings that can be tweaked and analyzed to investigate performance. The AKAZE algorithm and filtering steps have multiple parameters and settings that can likely be optimized for sensor, environment, and output quality.

The most important parameter from a military perspective is likely the speed to produce the co-registration. While the focus of this effort was the Auto-GCP pipeline and co-registration accuracy, the required pre- and post-processing steps consume a large majority of the processing time (greater than 90%). The ERDC-GRL team is actively investigating computational efficiencies that should address this problem. Specific techniques that are under study include the use of low-resolution frames within the initial mosaic generation and a generation of a coarse resolution DEM for the initial elevation extraction.

Additional functionality important to military applications would relate to the particular mission and specific devices to be used for geospatial exploitation. Often a reduced, derived, or subset of the data is all that is required for mission success. As an example, for mobility within urban environments, building geometry and other manmade features will be the critical data. In this application, segmentation approaches could reduce the amount of area selected for 3D generation and subsequent co-registration, which would improve the processing time and, potentially, co-registration accuracy. Interrelated, are the devices used by the military to accomplish the mission. New visualization and analytic equipment, such as targeting hardware, various heads-up display (HUD) devices, and the Integrated Visualization Augmentation System (IVAS), often makes use of wireframe models to accomplish required functions. Generation of wireframe data via 3D reconstruction can again be accomplished with a subset of data, and co-registration may be reduced to more efficient vector-based approaches.

Finally, while only briefly touched upon in the preceding sections, a critical component of the ERDC-GRL Auto-GCP pipeline is the use of the Agisoft Metashape software to perform the simultaneous bundle adjustment. ERDC-GRL has used other COTS and open source algorithms for this process and continues to monitor the photogrammetric community for additional capabilities and solutions. Ideally, a GOTS solution based on open source algorithms would be developed. Two software environments

under evaluation that could meet this need are COLMAP and ODM (native as well as NodeODM and WebODM implementations). These environments are currently undergoing testing using the same data as processed above and will be the subject of future communications.

6 Conclusion

The objective of this work was to develop procedures to automatically co-register tactical image data to 3D foundation products to meet the threats described by the MDO doctrine. The processing pipeline developed by ERDC-GRL integrated in-house code, open source software, and COTS tools. Four datasets from different sensors and locations were processed using foundation data obtained from NGA sources. Results showed that the co-registration of tactical drone data to reference foundation varied from 0.34 m to 0.75 m, exceeding the accuracy objective of 1 m described in briefings presented to the project stakeholders. Of particular importance was the ability to meet this metric with the ARTEMIS data over Afghanistan which covered over 4 km^2. Processing times for the co-registration step were judged acceptable, especially in comparison with the standard processing steps required for photogrammetric adjustment (10% or less of the total processing time budget). Finally, a discussion of efforts to improve processing efficiencies was noted to include image segmentation and optimization for specific applications.

References

Alcantarilla, P. F., A. Bartoli, and A. J. Davison. 2012. "KAZE Features." *European Conference on Computer Vision*. London: Imperial College, 214–227.

Alcantarilla, P. F., J. Nuevo, and A. Bartoli. 2011. "Fast Explicit Diffusion for Accelerated Features in Non-Linear Scale Spaces." *IEEE Transactions on Pattern Analysis and Machine Intelligence*: 1281–1298.

American Society of Photogrammetry and Remote Sensing. 2015. "ASPRS Positional Accuracy Standards for Digital Geospatial Data." *Photogrammetric Engineering and Remote Sensing* 81(3): A1–A26.

Grinston, M., J. McConville, and R. McCarthy. 2019. "Army Modernization Strategy: Investing in the Future." US Army TRADOC: 12.

James, M. R., J. H. Chandler, A. Eltner, C. Fraser, P. E. Miller, J. P. Mills, T. Noble, S. Robson, and S. N. Lane. 2019. "Guidelines on the Use of Structure-from-Motion Photogrammetry in Geomorphic Research." *Earth Surface Processes and Landforms* 44: 2081–2084. doi: https://doi.org/10.1002/esp.4637.

Lowe, D. G. 1999. "Object Recognition from Local Scale-Invariant Features." *Proceedings of the Seventh IEEE International Conference on Computer Visions:* 1150–1157.

Ruby, J. G., and R. D. Massaro. n.d. *Auto-GCP Registration Using PRI Data*. Final Report, Washington, DC: U.S. Army Corps of Engineers.

Schonberger, J. L., and J. Frahm. 2016. "Structure-from-Motion Revisited." *2016 IEEE Conference on Computer Vision and Pattern Recognition (CVPR)*: 4104–4113. doi:10.1109/CVPR.2016.445.

Secretary of the Army. 2017. "Army Directive 2017-22 (Implementation of Acquisition Reform Initiatives 1 and 2)."

Secretary of the Army. 2017. "Army Directive 2017-24 (Cross-Functional Team Pilot in Support of Material Development)."

Secretary of the Army. 2017. "Army Directive 2017-33 (Enabling the Army Modernization Task Force)."

Steffen, R., J. Frahm, and W Forstner. 2010. "Relative Bundle Adjustment Based on Trifocal Constraints." *European Conderence on Computer Vision*. Heraklion, Crete, Greece: Springer, 282–295.

U.S. Army. 2018. "TRADOC Pamphlet 525-3-1, The U.S. Army Multi-Domain Operations 2028," 100.

US Army Corps of Engineers. 2015. "Photogrammetric and LiDAR Mapping." Manual, 607.

Westoby, M. J., J. Brasington, N. F. Glasser, M. J. Hambrey, and J. M. Reynolds. 2012. "'Structure-from-Motion' Photogrammetry: A Low-Cost, Effective Tool for Geoscience Applications." *Geomorphology* 179: 300–314.

REPORT DOCUMENTATION PAGE

Form Approved
OMB No. 0704-0188

1. REPORT DATE *(DD-MM-YYYY)*	2. REPORT TYPE	3. DATES COVERED *(From – To)*
01-2023	Final Technical Report	

4. TITLE AND SUBTITLE

Three-Dimensional Geospatial Product Generation from Tactical Sources, Co-Registration Assessment, and Considerations

5a. CONTRACT NUMBER

5b. GRANT NUMBER

5c. PROGRAM ELEMENT NUMBER
0602146A

6. AUTHOR(S)

Jeffrey G. Ruby, Richard D. Massaro, John E. Anderson, Robert L. Fischer

5d. PROJECT NUMBER
AT7

5e. TASK NUMBER

5f. WORK UNIT NUMBER

7. PERFORMING ORGANIZATION NAME(S) AND ADDRESS(ES)

Geospatial Research Laboratory
U.S. Army Engineer Research and Development Center
7701 Telegraph Road
Alexandria, VA 22315

Strategic Alliance Consulting, Inc.
53A E. Lee Street
Warrenton, VA 20186

8. PERFORMING ORGANIZATION REPORT NUMBER

ERDC/GRL TR-23-1

9. SPONSORING / MONITORING AGENCY NAME(S) AND ADDRESS(ES)

Headquarters
U.S. Army Corps of Engineers
Washington, DC 20314-1000

10. SPONSOR/MONITOR'S ACRONYM(S)

USACE

11. SPONSOR/MONITOR'S REPORT NUMBER(S)

12. DISTRIBUTION / AVAILABILITY STATEMENT

Approved for public release; distribution is unlimited.

13. SUPPLEMENTARY NOTES

14. ABSTRACT

According to Army Multi-Domain Operations (MDO) doctrine, generating timely, accurate, and exploitable geospatial products from tactical platforms is a critical capability to meet threats. The US Army Corps of Engineers, **Engineer Research and Development Center,** Geospatial Research Laboratory (ERDC-GRL) is carrying out 6.2 research to facilitate the creation of three-dimensional (3D) products from tactical sensors to include full-motion video, framing cameras, and sensors integrated on small Unmanned Aerial Systems (sUAS). This report describes an ERDC-GRL processing pipeline comprising custom code, open-source software, and commercial off-the-shelf (COTS) tools to geospatially rectify tactical imagery to authoritative foundation sources. Four datasets from different sensors and locations were processed against National Geospatial-Intelligence Agency–supplied foundation data. Results showed that the co-registration of tactical drone data to reference foundation varied from 0.34 m to 0.75 m, exceeding the accuracy objective of 1 m described in briefings presented to Army Futures Command (AFC) and the Assistant Security of the Army for Acquisition, Logistics and Technology (ASA(ALT)). A discussion summarizes the results, describes steps to address processing gaps, and considers future efforts to optimize the pipeline for generation of geospatial data for specific end-user devices and tactical applications.

15. SUBJECT TERMS

Military planning; Military geography; Geospatial data--computer processing; Remote sensing; Remote-sensing images

16. SECURITY CLASSIFICATION OF:			17. LIMITATION OF ABSTRACT	18. NUMBER OF PAGES	19a. NAME OF RESPONSIBLE PERSON
a. REPORT	b. ABSTRACT	c. THIS PAGE			19b. TELEPHONE NUMBER *(include area code)*
Unclassified	Unclassified	Unclassified	None	53	